ISSN 0020-1685, Inorganic Materials, 2015, Vol. 51, No. 7, pp. 650–654. © Pleiades Publishing, Ltd., 2015.
Original Russian Text © L.T. Denisova, Yu.F. Kargin, L.A. Irtyugo, V.M. Denisov, 2015, published in Neorganicheskie Materialy, 2015, Vol. 51, No. 7, pp. 714–718.

Phase Relations in the Bi_2O_3–SnO_2 System and Thermodynamic Properties of Bismuth Pyrostannate

L. T. Denisova[a], Yu. F. Kargin[b], L. A. Irtyugo[a], and V. M. Denisov[a]

[a] *Institute of Nonferrous Metals and Materials Science, Siberian Federal University, Svobodnyi pr. 79, Krasnoyarsk, 660041 Russia*

[b] *Baikov Institute of Metallurgy and Materials Science, Russian Academy of Sciences, Leninskii pr. 49, Moscow, 119991 Russia*

e-mail: antluba@mail.ru

Received December 10, 2014

Abstract—Phase relations in the Bi_2O_3–SnO_2 system have been studied using differential thermal analysis, differential scanning calorimetry, X-ray diffraction, and the sessile drop method. The $C_p(T)$ curve obtained in the range 350–960 K has a number of extrema, which are attributable to structural changes in $Bi_2Sn_2O_7$. The experimental C_p data have been used to evaluate the thermodynamic properties of the oxide compound.

DOI: 10.1134/S0020168515070043

INTRODUCTION

Bismuth pyrostannate, $Bi_2Sn_2O_7$, has attracted researchers' attention because it combines unique properties, which allow it to be employed as a catalyst, a sensitive material in gas sensors for carbon monoxide detection in the presence of other gases, etc. [1–7]. At the same time, there are very limited and, in a number of cases, contradictory data on the properties of $Bi_2Sn_2O_7$. This refers primarily to phase equilibrium data for the Bi_2O_3–SnO_2 system. Three phase diagrams of this system have been reported to date [1, 8–10]. According to early studies [8], the Bi_2O_3–SnO_2 system contains only one compound, $Bi_2Sn_2O_7$, which melts congruently at 1638 K and undergoes solid-state decomposition at temperatures below 873 K. According to Kargin et al. [1], $Bi_2Sn_2O_7$ melts congruently at 1678 K and is stable at temperatures below 873 K. Note that, in their study, all experiments were carried out in platinum crucibles. The Bi_2O_3 + $Bi_2Sn_2O_7$ eutectic was found to contain 2 mol % SnO_2 and melt at 1098 K.

Asryan et al. [9, 10] carried out their experiments in alundum crucibles. According to their results, the eutectic contains ≃6 mol % SnO_2 and melts at 1033 K, and the $Bi_2Sn_2O_7$ compound melts incongruently at 1573 K. Their $Bi_2Sn_2O_7$ samples contained 0.19 at % Al after solid-state synthesis in alundum crucibles and 2.15 at % Al after differential thermal analysis (DTA) scans. It cannot be ruled out that the distinction of their results from what was reported by Kargin et al. [1] was due to contamination of the Bi_2O_3–SnO_2 samples with aluminum. Denisov et al. [11] examined the effect of interaction with Al_2O_3 crucibles on the properties of synthesized oxides using the PbO–GeO_2 system as an example (PbO is similar in reactivity to Bi_2O_3). Lead germanate samples were synthesized in Al_2O_3 and BeO crucibles, and the GeO_2 content was varied from 25 to 60 mol %. In all cases, glassy materials were obtained in the Al_2O_3 crucibles. The materials obtained in the BeO crucibles were glassy at 50 and 60 mol % GeO_2; glassy with crystalline inclusions at 33.2, 37.5, and 40 mol % GeO_2; and crystalline at 25 mol % GeO_2. X-ray fluorescence analysis of 75 mol % PbO + 25 mol % GeO_2 glass indicated the presence of 3.15 wt % Al_2O_3. This led Denisov et al. [11] to conclude that the synthesis of PbO–GeO_2 materials in alundum crucibles was accompanied by doping with aluminum oxide. This was assumed to be responsible for the formation of glassy PbO–GeO_2 materials in Al_2O_3 crucibles. Clearly, interaction of Bi_2O_3–SnO_2 samples with alumina (crucible material) influences the behavior of this system.

According to Shannon et al. [3], the $Bi_2Sn_2O_7$ compound exists in three polymorphs: α-$Bi_2Sn_2O_7$ (tetragonal cell: a = 21.328 Å, c = 21.545 Å) is stable below 363 K; β-$Bi_2Sn_2O_7$ (cubic cell: a = 21.40 Å) has a temperature stability range from 363 to 953 K; and γ-$Bi_2Sn_2O_7$ (face-centered cubic cell: a = 10.73 Å) is stable at temperatures above 953 K. According to Roth [12], the structure of $Bi_2Sn_2O_7$ is similar to a distorted cube. Nevertheless, the true symmetry of its crystal lattice is not cubic. According to Vetter et al. [13], $Bi_2Sn_2O_7$ has a distorted pyrochlore structure (tetragonal lattice: a = 21.31 Å, c = 21.53 Å).

Asryan et al. [9] were the first to report that the $Bi_2Sn_2O_7$ compound had an orthorhombic structure:

a = 12.262 Å, b = 3.765 Å, and c = 7.957 Å. Later, Udod et al. [14] obtained similar lattice parameters of this phase.

The lattice parameter of γ-$Bi_2Sn_2O_7$ has been variously reported to be a = 10.7435(1) [4], 10.7225(7) [15], or 10.76 Å [16].

According to Walsh and Watson [16], the lattice parameters of α-$Bi_2Sn_2O_7$ are a = 15.34 Å and c = 21.74 Å, whereas Evans et al. [17] reported a = 15.0502(6) Å, b = 15.0545(6) Å, c = 21.5114(4) Å, and β = 90.038(4)°.

There is currently very little data on the thermodynamic properties of the Bi_2O_3–SnO_2 system. Asryan et al. [9, 10] carried out a thermodynamic study of this system using effusion measurements in combination with mass spectrometric analysis of the vapor phase in the temperature range from 1000 to 1270 K. The thermodynamic properties of $Bi_2Sn_2O_7$ reported by Belousova and Arkhipova [18] were assessed using semiempirical methods. In addition, its heat capacity was determined experimentally by differential scanning calorimetry (DSC) (300–1000 K). Roy et al. [19] reported the heat capacity of $Bi_2Sn_2O_7$ in the temperature range 523–843 K [19].

The objectives of this work were to study phase relations in the Bi_2O_3–SnO_2 system using X-ray diffraction, DTA, DSC, and the sessile drop method and assess the thermodynamic properties of $Bi_2Sn_2O_7$.

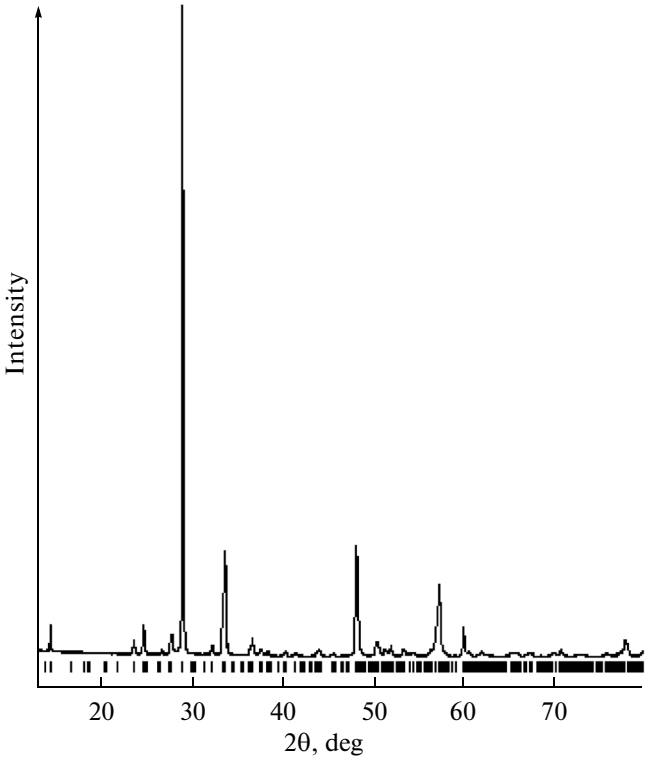

Fig. 1. Room-temperature X-ray diffraction pattern of $Bi_2Sn_2O_7$.

EXPERIMENTAL

Given some specific features of the phase equilibria in the Bi_2O_3–SnO_2 system and the high reactivity of liquid bismuth oxide, $Bi_2Sn_2O_7$ was prepared by solid-state reaction. The starting chemicals used were Bi_2O_3 (extrapure grade, OSCh 13-3) and SnO_2 (reagent grade). The individual oxides were first precalcined in air at 873 K. A stoichiometric mixture of the oxides was ground in an agate mortar and then pressed. The resultant green compacts were fired in air at 1003 K for 30 h with intermediate grindings every 5 h. The solid-state synthesis temperature was chosen with allowance for the following factors: (1) at this temperature, the monoclinic phase α-Bi_2O_3 undergoes a polymorphic transformation into the high-temperature phase δ-Bi_2O_3 [20], and (2) crystallographic transformations improve the reactivity of solids (Hedvall effect) [21, 22]. The phase composition of the samples thus prepared was determined by X-ray diffraction on an X'Pert Pro MPD diffractometer (PANalytical, Netherlands) with CuK_α radiation. X-ray diffraction patterns were collected using a PIXcel fast detector in the angular range 13°–123° with a scan step of 0.013°. The data obtained are presented in Fig. 1. Lattice parameters were determined by profile fitting using derivative difference minimization [23]. At room temperature, the synthesized $Bi_2Sn_2O_7$ samples had the following unit-cell parameters: $a = b$ = 15.1026(9) Å, c = 21.515(2) Å (tetragonal symmetry, sp. gr. $I\bar{4}c2$ (8)). Therefore, our results agree better with those reported by Evans et al. [17].

Molar heat capacity C_p was measured using a Netzsch STA 449 C Jupiter system and platinum crucibles. In our experiments, we used specially designed holders for heat capacity measurements. The experimental procedure was described in detail elsewhere [24, 25]. Given some specific features of the behavior of $Bi_2Sn_2O_7$ in a carbon monoxide atmosphere, the measurements were performed in an argon atmosphere. The experimental data were analyzed using the Netzsch Proteus Thermal Analysis software package and licensed Systat Sigma Plot 12 graphing software. The temperature range of high-temperature heat capacity measurements was chosen based on preliminary differential thermal analysis data.

The interaction of Bi_2O_3–SnO_2 melts containing 0–5 mol % SnO_2 with a solid SnO_2 substrate was studied by the sessile drop method, with the sample and substrate heated separately. The experimental procedure was similar to that described previously [26].

RESULTS AND DISCUSSION

Figure 2 illustrates the temperature effect on the heat capacity of $Bi_2Sn_2O_7$. It is seen that C_p increases with increasing temperature and that the $C_p(T)$ curve has a well-defined peak centered at T = 898 K. Previous data [3] indicate that the observed peak arises from

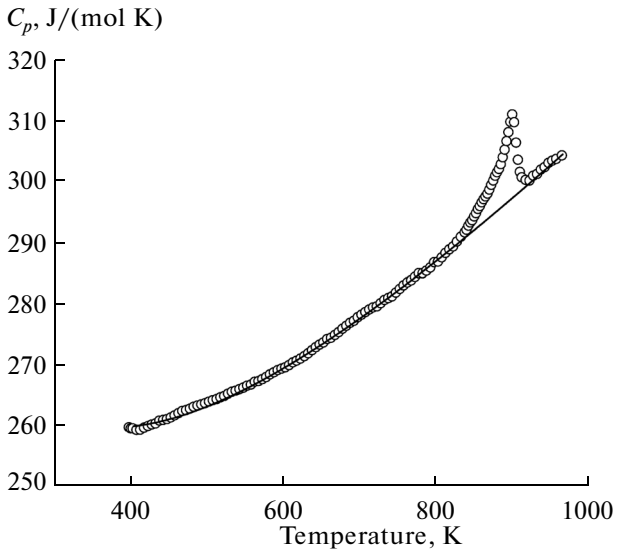

Fig. 2. Heat capacity as a function of temperature for $Bi_2Sn_2O_7$. The open circles represent the experimental data and the solid line represents a theoretical fit.

the β-$Bi_2Sn_2O_7 \rightarrow \gamma$-$Bi_2Sn_2O_7$ phase transition. The continuous variation in the heat capacity of $Bi_2Sn_2O_7$ around the peak suggests that the transition is second-order [27–29]. At the same time, the peak is lambda-shaped, demonstrating that the heat capacity of $Bi_2Sn_2O_7$ in the region of the transition is influenced by thermodynamic fluctuations. The jump in C_p in the region of the phase transition is $\Delta C_p(T_{max}) \simeq 13$ J/(mol K), and the transition width is $\Delta T \simeq 80$ K. The ΔT value is rather high, which also suggests that the transition is second-order (In the case of first-order phase transitions, the peak in heat capacity is very narrow and its width is typically less than 10 K [29]). According to Gusev [29], the large width of the peak may be due to the sluggish kinetics of the transition. At the same time, the wide temperature range of the peak reflects the changes in short-range order that gradually occur in the vicinity of the phase transition. It has been proposed [29] that, to gain greater insight into this effect, C_p measurements in the vicinity of the phase transition should be made at various temperature scan rates. In our experiments, C_p was measured at a heating rate of 10 or 20 K/min with a 0.5-K step size, and we obtained identical results.

The entropy of a phase transition can be evaluated from experimental $C_p(T)$ data obtained in a wide temperature range that includes the temperature of the phase transition [30]. To this end, the excess heat capacity C_{p_i} of the phase transition is determined as the difference between the measured heat capacity and its regular part C_b, represented by the baseline of the $C_p(T)$ curve [31]. The baseline was determined by extrapolating the heat capacity below the transition (842 K) to the high-temperature region (922 K).

For these conditions, evaluation of the transition ΔS from the excess heat capacity in the region of the phase transition gives $\Delta S = \int (C_{p_i} - C_b)\, dT/T \simeq 0.4$ J/(mol K).

Note that the $C_p(T)$ curves of all the synthesized $Bi_2Sn_2O_7$ samples showed a small peak near 363 K. Its position coincides with the temperature of the α-$Bi_2Sn_2O_7 \rightarrow \beta$-$Bi_2Sn_2O_7$ polymorphic transformation, identified by Shannon et al. [3].

Since the polymorphic transformations of bismuth stannate are accompanied by very small changes in its heat capacity, these were left out of consideration in describing the temperature dependence of its C_p. With no allowance for the changes induced by the phase transitions, the temperature-dependent heat capacity data for $Bi_2Sn_2O_7$ can be represented by the equation [32]

$$C_p = a + bT + cT^{-2} + dT^{-0.5}. \quad (1)$$

For $Bi_2Sn_2O_7$ in the temperature range 400–950 K, it has the form

$$C_p = 94.82 + 0.146T - 0.0015T^{-2} + 2133.53T^{-0.5}. \quad (2)$$

The correlation coefficient for Eq. (2) was determined to be $r = 0.9996$. It is worth noting that, using other known equations of temperature-dependent heat capacity [33] for describing the present $C_p(T)$ data for the $Bi_2Sn_2O_7$ compound, we obtained less satisfactory results. According to Walsh et al. [34], $Bi_2Sn_2O_7$ has one of the most complex crystal structures among oxide compounds characterized by X-ray powder diffraction. Clearly, the observed polymorphic transformations and specific features of the associated distortions of this structure determine the shape of the $C_p(T)$ curve above room temperature.

The temperature effect on the molar heat capacity of $Bi_2Sn_2O_7$ was reported by Belousova and Arkhipova [18]. Since neither the structural characteristics of their samples nor synthesis conditions were specified in their report [18], their results cannot be compared to ours. We can only note the atypical $C_p(T)$ behavior and the high absolute values of C_p (at $T = 900$ K, the difference in C_p values is as large as $\simeq$100 J/(mol K)).

Using Eq. (2) in combination with well-known thermodynamic relations, we determined the enthalpy increment $H^0(T) - H^0(400\text{ K})$ and entropy change $S^0(T) - S^0(400\text{ K})$. The results are presented in the table.

Given that wetting in an equilibrium system leads to finite contact angles and that, when the melt composition varies along the liquidus line, the eutectic melt has the largest contact angle [35], we investigated the wetting of SnO_2 by Bi_2O_3–SnO_2 melts containing up to 5 mol % SnO_2. It is remarkable that, at a temperature corresponding to its melting point, molten Bi_2O_3 brought into contact with a SnO_2 substrate immediately spreads over the surface, without forming finite

Thermodynamic properties of $Bi_2Sn_2O_7$

T, K	C_p, J/(mol K)	$H^0(T) - H^0(400\ K)$, kJ/mol	$S^0(T) - S^0(400\ K)$, J/(mol K)	$\Phi^0(T)$, J/(mol K)
400	259.9	–	–	–
450	261.1	13.02	30.67	1.34
500	263.2	26.12	58.28	6.04
550	266.1	39.36	83.50	11.94
600	269.5	52.74	106.8	18.90
650	273.4	66.31	128.5	26.50
700	277.6	80.09	148.9	34.52
750	282.2	94.09	168.2	42.79
800	287.0	108.3	186.6	51.23
850	292.1	122.8	204.2	59.73
900	297.3	137.5	221.01	68.22
950	302.7	152.5	237.2	76.67

contact angles. According to Naidich et al. [36], complete wetting and a positive spreading coefficient K_s,

$$K_s = W_a - W_c = \sigma(\cos\theta - 1), \quad (3)$$

mean that

$$\sigma_{sv} > \sigma_{sl} + \sigma_{lv}. \quad (4)$$

In (3) and (4), W_a and W_c are the works of adhesion and cohesion, respectively; σ_{sv}, σ_{sl}, and σ_{lv} are the solid–vapor, solid–liquid, and liquid–vapor surface tension coefficients, respectively; and θ is the contact angle. In addition to wetting, the formation of contacts between solid and liquid phases in nonequilibrium systems (in our instance, $Bi_2O_3(l)$–$SnO_2(s)$ is followed by interfacial processes that equalize the chemical potentials of the components of the liquid and solid phases (dissolution of the substrate in the melt, diffusion from the liquid phase to the substrate, and others) [37]. Like pure Bi_2O_3, immediately after being brought into contact with SnO_2 at temperatures corresponding to the liquidus of the Bi_2O_3–SnO_2 system, the melts containing up to 5 mol % SnO_2 spread over the substrate, without forming steady-state contact angles. Therefore, in this case as well there is good adhesion in the melt–substrate system. Because of this circumstance, we were unable to more accurately determine the position of the eutectic in the Bi_2O_3–SnO_2 system by the method in question.

CONCLUSIONS

Phase relations in the Bi_2O_3–SnO_2 system have been studied using differential thermal analysis, X-ray diffraction, and the sessile drop method. The molar heat capacity of $Bi_2Sn_2O_7$ has been determined by differential scanning calorimetry. The $C_p(T)$ curve obtained in the range 350–960 K has extrema at 363 and 898 K, which are due to the polymorphic transformations of $Bi_2Sn_2O_7$. The experimental $C_p(T)$ data have been used to evaluate the thermodynamic properties of bismuth pyrostannate: the enthalpy increment $H^0(T) - H^0(400\ K)$ is 13.02 and 152.5 kJ/mol at 450 and 950 K, respectively, and the entropy change $S^0(T) - S^0(400\ K)$ is 30.67 and 237.2 J/(mol K) at 450 and 950 K, respectively.

ACKNOWLEDGMENTS

This work was supported in part by the RF Ministry of Education and Science (state research target for Siberian Federal University).

REFERENCES

1. Kargin, Yu.F., Nelyapina, N.I., and Skorikov, V.M., System Bi_2O_3–SnO_2, in *Fiziko-khimicheskie issledovaniya ravnovesii v rastvorakh* (Physicochemical Studies of Equilibria in Solutions), Yaroslavl: YaGRI im. K.D. Ushinskogo, 1988, pp. 81–83.
2. Mao, Y., Li, G., Xu, W., et al., Hydrothermal synthesis and characterization of nanocrystalline pyrochlore oxides $M_2Sn_2O_7$ (M = La, Bi, Gd or Y), *J. Mater. Chem.*, 2000, vol. 10, pp. 479–482.
3. Shannon, R.D., Bierlein, J.D., Gillson, J.L., et al., Polymorphism in $Bi_2Sn_2O_7$, *J. Phys. Chem. Solids*, 1980, vol. 41, pp. 117–122.
4. Jones, R.H. and Knight, K.S., The structure of γ-$Bi_2Sn_2O_7$ at 725°C by high-resolution neutron diffraction: implications for bismuth(III)-containing pyrochlores, *J. Chem. Soc., Dalton Trans.*, 1977, pp. 2551–2555.
5. Moens, L., Ruiz, P., Delmon, B., et al., Cooperation effects towards partial oxidation of isobutene in multiphasic catalysts based on bismuth pyrostannate, *Appl. Catal., A*, 1998, vol. 171, pp. 131–143.

6. Mims, C.A., Jacobson, A.J., Hall, R.B., et al., Methane oxidative coupling over nonstoichiometric bismuth–tin pyrochlore catalysts, *J. Catal.*, 1995, vol. 153, pp. 197–207.
7. Devi, G.S., Manorama, S.V., and Rao, V.J., SnO_2/Bi_2O_3: a suitable system for selective carbon monoxide detection, *J. Electrochem. Soc.*, 1988, vol. 145, no. 3, pp. 1039–1044.
8. *Diagrammy sostoyaniya sistem tugoplavkikh oksidov: Spravochnik* (Phase Diagrams of Refractory Oxide Systems: A Handbook), issue 5: *Dvoinye sistemy* (Binary Systems), Galakhov, F.Ya., Ed., Leningrad: Nauka, 1986, part 2, pp. 298–299.
9. Asryan, N.A., Kol'tsova, T.N., Alikhanyan, A.S., and Nipan, G.D., Thermodynamics and phase diagram of the Bi_2O_3–SnO_2 system, *Inorg. Mater.*, 2002, vol. 38, no. 11, pp. 1141–1147.
10. Asryan, N.A., Kol'tsova, T.N., Alikhanyan, A.S., and Nipan, G.D., Phase equilibria in the Bi_2O_3–SnO_2 system, *Russ. J. Phys. Chem. A*, 2003, vol. 77, no. 11, pp. 1740–1744.
11. Denisov, V.M., Kuchumova, O.V., Denisova, L.T., et al., Contact interaction of PbO–GeO_2 melts with silver, *Rasplavy*, 2010, no. 1, pp. 3–8.
12. Roth, R.S., Pyrochlore-type compounds containing double oxides of trivalent and tetravalent ions, *J. Res. Natl. Bur. Stand.*, 1956, vol. 56, pp. 17–25.
13. Vetter, G., Queyroux, F., and Gilles, J.-C., Preparation, stabilite et etude cristallographique preliminaire du compose $Bi_2Sn_2O_7$, *Mater. Res. Bull.*, 1978, vol. 13, pp. 211–216.
14. Udod, L.V., Aplesnin, S.S., Sitnikov, M.N., and Molokoev, M.S., Dielectric and electrical properties of polymorphic bismuth pyrostannate $Bi_2Sn_2O_7$, *Phys. Solid State*, 2014, vol. 56, no. 7, pp. 1315–1319.
15. Kahlenberg, V. and Zeiske, Th., Structure of γ-$Bi_2Sn_2O_7$ by high-temperature powder neutron diffraction, *Z. Kristallogr.*, 1997, vol. 212, no. 4, pp. 297–301.
16. Walsh, A. and Watson, G.W., Polymorphism in bismuth stannate: a first-principles study, *Chem. Mater.*, 2007, vol. 19, pp. 5158–5164.
17. Evans, I.R., Howard, J.A.K., and Evans, S.O., α-$Bi_2Sn_2O_7$—a 176 atom crystal structure from powder diffraction, *J. Mater. Chem.*, 2003, vol. 13, pp. 2098–2103.
18. Belousova, N.V. and Arkhipova, E.O., Thermodynamic properties of bismuth pyrostannate, *Polzunovsk. Vestn.*, 2009, no. 3, pp. 56–59.
19. Roy, M., Bala, I., and Barbar, S.K., Synthesis, structural, electrical and thermal properties of Ti-doped $Bi_2Sn_2O_7$, *J. Therm. Anal. Calorim.*, 2012, vol. 110, pp. 559–565.
20. Kargin, Yu.F., Burkov, V.I., Mar'in, A.A., et al., *Kristally $Bi_{12}M_xO_{20\pm\delta}$ so strukturoi sillenita. Sintez, stroenie, svoistva* (Sillenite-Structure $Bi_{12}M_xO_{20\pm\delta}$ Crystals: Synthesis, Structure, and Properties), Moscow: Inst. Obshchei i Neorgsnicheskoi Khimii Ross. Akad. Nauk, 2004.
21. Tret'yakov, Yu.D. and Putlyaev, V.I., *Vvedenie v khimiyu tverdofaznykh materialov* (Introduction to the Chemistry of Solid Materials), Moscow: Mosk. Gos. Univ., Nauka, 2006.
22. Tret'yakov, Yu.D., *Tverdofaznye reaktsii* (Solid-State Reactions), Moscow: Khimiya, 1978.
23. Solovyov, L.A., Full-profile refinement by derivative difference minimization, *J. Appl. Crystallogr.*, 2004, vol. 37, pp. 743–749.
24. Denisov, V.M., Denisova, L.T., Irtyugo, L.A., and Biront, V.S., Thermal physical properties of $Bi_4Ge_3O_{12}$ single crystals, *Phys. Solid State*, 2010, vol. 52, no. 7, pp. 1362–1365.
25. Denisova, L.T., Kargin, Yu.F., Chumilina, L.G., et al., High-temperature heat capacity of $Sc_2Cu_2O_5$, *Inorg. Mater.*, 2014, vol. 50, no. 5, pp. 482–484.
26. Denisova, L.T., Krinitsyn, D.O., Denisov, V.M., et al., Wetting of the noble metals by Bi_2O_3–CaO melts, *Rasplavy*, 2014, no. 5, pp. 3–6.
27. Vonsovskii, S.V., *Magnetizm* (Magnetism), Moscow: Nauka, 1971.
28. Potashinskii, A.Z. and Pokrovskii, V.L., *Fluktuatsionnaya teoriya fazovykh perekhodov* (Fluctuation Theory of Phase Transitions), Moscow: Nauka, 1982.
29. Gusev, A.I., *Nestekhiometriya, besporyadok, blizhnii i dal'nii poryadok v tverdom tele* (Nonstoichiometry, Disorder, and Short- and Long-Range Order in Solids), Moscow: Fizmatlit, 2007.
30. Strukov, B.A. and Levanyuk, A.P., *Fizicheskie osnovy segnetoelektricheskikh yavlenii v kristallakh* (Physical Principles of Ferroelectricity in Crystals), Moscow: Fizmatlit, 1983.
31. Bush, A.A. and Popova, E.A., Heat capacity of the $Pb_5(Ge_{1-x}Si_x)_3O_{11}$ ferroelectric system, *Phys. Solid State*, 2004, vol. 46, no. 5, pp. 902–907.
32. Holland, T.J.B. and Powell, R., An enlarged and updated internally consistent thermodynamic dataset with uncertainties and correlations: the system K_2O–FeO–Fe_2O_3–Al_2O_3–TiO_2–SiO_2–C–H_2–O_2, *J. Metamorph. Geol.*, 1990, vol. 8, pp. 89–124.
33. Chudnenko, K.V., *Termodinamicheskoe modelirovanie v geokhimii: teoriya, algoritmy, programmnoe obespechenie, prilozheniya* (Thermodynamic Modeling in Geochemistry: Theory, Algorithms, Software, and Applications), Novosibirsk: Geo, 2010.
34. Walsh, A., Watson, G.W., Payne, D.J., et al., A theoretical and experimental study of the distorted pyrochlore $Bi_2Sn_2O_7$, *J. Mater. Chem.*, 2006, vol. 16, pp. 3452–3458.
35. Naidich, Yu.V., Perevertailo, V.M., and Obushchak, L.P., Properties of solid–liquid interfaces in binary alloy crystallization processes, in *Adgeziya rasplavov* (Melt Adhesion), Kiev: Naukova Dumka, 1974, pp. 27–32.
36. Naidich, Yu.V., Perevertailo, V.M., Lebovich, E.M., et al., Interfacial and capillary phenomena in unary crystal–melt systems, in *Adgeziya rasplavov* (Melt Adhesion), Kiev: Naukova Dumka, 1974, pp. 3–7.
37. Summ, B.D. and Goryunov, Yu.V., *Fiziko-khimicheskie osnovy smachivaniya i rastekaniya* (Physicochemical Principles of Wetting and Spreading), Moscow: Khimiya, 1976.

Translated by O. Tsarev